Destruction of Quantum Coherence and Wave Packet Dynamics

Article · November 1998

Source: CiteSeer

CITATIONS
0

READS
29

3 authors, including:

G. Alber
Technische Universität Darmstadt
178 PUBLICATIONS **3,747** CITATIONS

SEE PROFILE

Destruction of quantum coherence and wave packet dynamics

Gernot Alber
Abteilung für Quantenphysik, Universität Ulm, D-89069 Ulm, Germany
(to be published in *The Physics and Chemistry of Wave Packets*, edited by J. A. Yeazell and T. Uzer (Wiley, N. Y.))

The development of short, powerful laser pulses and of sophisticated trapping techniques within the last few years has stimulated numerous theoretical and experimental investigations on the dynamics of wave packets in elementary, material quantum systems. These wave packets are non stationary, spatially localized quantum states which are situated on the border between the microscopic and macroscopic domain. A detailed understanding of their dynamics is essential for our conception of quantum mechanics and of its connection with classical mechanics. So far the interplay between classical and quantum mechanical aspects of their dynamics have been investigated in Rydberg systems (Alber and Zoller 1991), in molecules (Garraway and Suominen 1995, Sepulveda and Grossmann 1996), in clusters (Knospe and Schmidt 1996) and in nano structures (Koch et al. 1996). These studies have concentrated mainly on semiclassical aspects which may be attributed to the smallness of the relevant de Broglie wave lengths. Thereby quantum aspects still manifest themselves in interferences between probability amplitudes which are associated with various families of classical trajectories. However, for a comprehensive understanding of the emergence of classical behavior also a detailed understanding of the destruction of quantum coherence is required. Typically this destruction of coherence arises from external stochastic forces or environmental influences which cannot be suppressed. Though by now many aspects of the coherent dynamics of these wave packets are understood to a satisfactory degree still scarcely anything is known about the influence of destruction of quantum coherence.

The main aim of this article is to discuss characteristic physical phenomena which govern the destruction of quantum coherence of material wave packets. For systematic investigations on this problem it is advantageous to deal with physical systems in which wave packets can be prepared and detected in a controlled way and in which the mechanisms causing the destruction of quantum coherence can be influenced to a large extent. Rydberg atoms (Seaton 1983, Fano and Rau 1986) are paradigms of elementary quantum systems which meet these requirements. The high level density of Rydberg states close to an ionization threshold is particularly convenient for the experimental preparation of spatially localized electronic wave packets by coherent superposition of energy eigenstates (Alber and Zoller 1991). Furthermore, the dynamics of electronic Rydberg wave packets exhibits universal features which apply to atomic and molecular Rydberg wave packets as well as to Rydberg wave packets in more complex systems such as clusters. This dynamical universality might be traced

back to the fact that almost over its whole classically accessible range the dynamics of a Rydberg electron is governed by the Coulomb potential of the positively charged ionic core. This universality together with the fact that Rydberg systems are amenable to a systematic theoretical description with the help of semiclassical methods makes them attractive for theoretical investigations. In recent years many detailed investigations have been performed concerning various fundamental aspects of the coherent dynamics of Rydberg wave packets, such as the influence of core scattering processes (Alber 1989, Dando et al. 1995, Hüpper et al. 1995), the connection between classical bifurcation phenomena and quantum dynamics (Beims and Alber 1993, 1996, Main et al. 1994), the influence of the stimulated light force on the atomic center of mass motion (Alber 1992, Alber and Strunz 1994) or the influence of electron correlations on wave packet dynamics in laser-induced two-electron excitation processes (Hanson and Lambropoulos 1995, Zobay and Alber 1995, van Druten and Muller 1995).

The dynamics of Rydberg electrons is governed by characteristic features which greatly influence the way in which they can be affected by external stochastic forces or environments. Most notably, Rydberg electrons can be influenced by laser fields of moderate intensities and by their statistical properties only in a small region around the atomic nucleus (Giusti and Zoller 1987). Furthermore, Rydberg systems are characterized by unique threshold phenomena which result from the infinitely many bound states and from the continuum states converging towards an ionization threshold. In addition, radiative decay rates of Rydberg states are so small that in typical situations of current experimental interest the direct influence of radiative damping can be neglected. However, the dissipative influence of radiative decay might become significant, if Rydberg systems interact with intense laser fields. In order to demonstrate characteristic physical phenomena governing the destruction of quantum coherence of electronic Rydberg wave packets in the subsequent discussion two stochastic mechanisms will be considered in detail, namely radiative damping which is mediated by electron correlations between a Rydberg wave packet and a resonantly excited, tightly bound core electron and fluctuations of laser fields.

The investigation of radiative damping mediated by electron correlation effects is motivated by the recently revived interest in laser-induced two electron excitation processes (Jones and Bucksbaum 1991, Stapelfeldt et al. 1991, Robicheaux 1993, Grobe and Eberly 1993, Hanson and Lambropoulos 1995, Zobay and Alber 1995, van Druten and Muller 1995). Non-resonant laser-induced excitation processes in which two valence electrons of an atom, e.g. an alkaline earth atom, are excited simultaneously have already been playing an important role in spectroscopy for a long time (Gallagher 1994). Typically thereby one of the valence electrons is excited into a Rydberg state and the other one into a tightly bound core state. Due to the availability of intense laser light sources recently also cases have become accessible experimentally in which both of these electrons are excited resonantly so that the influence of the laser field can no longer be treated with the help of perturbation theory. The resulting strong modifica-

tions of the electron-correlations may give rise to interesting novel phenomena. If the Rydberg electron is prepared in a wave packet state these coherent laser-modified electron correlations may even lead to an almost complete suppression of autoionization (Hanson and Lambropoulos 1995). In the subsequent discussion it will be demonstrated that these coherent effects are rather sensitive to the destruction of coherence which is caused by radiative decay of the tightly bound, excited core electron.

Due to the inherent stochastic nature of laser light the investigation of optical excitations of atoms or molecules by fluctuating laser fields is one of the central problems of laser spectroscopy. So far research on this problem has concentrated predominantly on laser-induced excitation of isolated energy eigenstates (Agarwal 1976, Dixit et al 1980, Vemuri et al. 1991). By now this special class of excitation processes is understood to a satisfactory degree. Despite these successes so far scarcely anything is known about the effect of laser fluctuations on optical excitation processes in which the level density of the resonantly excited states is large and in which wave packets are prepared. A paradigm in this respect is the laser-induced excitation of Rydberg and continuum states close to an ionization threshold which typically leads to the preparation of an electronic Rydberg wave packet. This physical system is well suited for investigating fundamental aspects of the destruction of quantum coherence on wave packet dynamics. In the subsequent discussion it will be demonstrated that this fluctuation-induced destruction of quantum coherence together with the peculiar threshold phenomena of Rydberg systems leads to a variety of novel phenomena. One of these generic effects is stochastic ionization which manifests itself in a characteristic scenario of non-exponential decays (Alber and Eggers 1997).

This paper is organized as follows: In section 1 basic theoretical concepts for describing the dynamics of Rydberg electrons in laser fields are summarized. This section focuses on coherent dynamical aspects which can be described conveniently with the help of semiclassical methods. Within this framework quantum aspects manifest themselves in the interference between probability amplitudes which are associated with those classical trajectories along which probability is transported. In section 2 recent theoretical work on the destruction of quantum coherence in wave packet dynamics is reviewed. Characteristic phenomena are exemplified by considering two dissipative mechanisms in detail. In section 2.1 the influence of radiative damping on laser-induced two-electron excitation processes is investigated. Effects of laser fluctuations on the dynamics of electronic Rydberg wave packets are discussed in Sec. 2.2.

1 Coherent dynamics of Rydberg electrons - general theoretical concepts

In this section a brief review of general theoretical concepts is presented which are useful for the description of the dynamics of Rydberg electrons. These concepts have already been used successfully to describe various aspects of the coherent dynamics of electronic Rydberg wave packets. Thereby we shall concentrate mainly on cases of recent experimental and theoretical interest in which a weakly bound Rydberg electron interacts with a laser field and additional weak electric and/or magnetic fields (Alber 1989, Dando et al. 1995, Hüpper et al. 1995, Moser et al. 1997). Throughout this review Hartree atomic units will be used for which $e = \hbar = m_e = 1$ (e and m_e are the electronic charge and mass, respectively).

Rydberg electrons are atomic or molecular electrons whose dynamics is dominated by highly excited energy eigenstates close to an ionization threshold. In the simplest possible case the energies of these Rydberg states are given by the well known relation $\epsilon_n = -1/[2(n-\alpha)^2]$ (Seaton 1983, Fano and Rau 1986). Thereby the quantum defect α is approximately energy independent for energies sufficiently close to the ionization threshold at energy $\epsilon = 0$. In typical optical excitation processes only Rydberg states with small values of the angular momentum l are excited, i.e. $l \ll n$. These Rydberg states of low angular momenta are essentially de-localized over the whole space which is classically accessible to them, i.e. $(l+1/2)^2 < r < 1/\mid \epsilon_n \mid$. ($r$ denotes the radial distance of the electron from the nucleus measured in units of the Bohr radius $a_0 = 5.29 \times 10^{-11}$m.)

If a Rydberg electron interacts with a laser field of moderate intensity and with a weak, static electric and/or magnetic field one can distinguish three characteristic spatial regimes:

(1) *The core region:* $(0 < r < O(1))$

It extends a few Bohr radii around the atomic nucleus. Inside this core region Rydberg electrons of low angular momenta which are able to penetrate this core region interact with all other atomic core electrons. These interactions lead to characteristic electron correlations effects such as autoionization and channel coupling. Quantitatively these effects can be described by quantum defect parameters which are approximately energy independent close to an ionization threshold (Seaton 1983, Fano 1986, Aymar et al. 1996).

If a Rydberg electron of low angular momentum interacts with a laser field of moderate intensity, whose electric field strength is given by

$$\mathbf{E}(t) = \mathbf{E}_0 e^{-i\omega t} + c.c., \tag{1}$$

two major effects take place. Firstly, the Rydberg electron experiences an intensity dependent ponderomotive energy shift of magnitude $\delta\omega_p = \mid \mathbf{E}_0 \mid^2 /\omega^2$. This

energy shift is independent of the energy of the Rydberg electron and may thus be interpreted as an energy shift of the ionization threshold. Secondly, all other dominant energy exchange processes between a Rydberg electron and the laser field are localized within a region typically extending a few Bohr radii around the atomic nucleus. This localization of the electron-laser coupling inside the core region relies on two sufficient conditions, namely moderate laser intensities and sufficiently high laser frequencies preferably in the optical frequency domain (Giusti and Zoller 1987). Thereby laser intensities are considered to be moderate provided the stationary oscillation amplitude α_{osc} of an electron in the laser field (in the absence of the Coulomb potential of the ionic core) is significantly less than the extension of the core region, i.e.

$$\alpha_{osc} = \mid \mathbf{E}_0 \mid /\omega^2 \ll 1. \tag{2}$$

Furthermore, in this context laser frequencies ω are considered to be high, if they are much larger than the inverse classical Kepler period T_n of the Rydberg electron, i.e. $\omega T_n \gg 1$ with $T_n = 2\pi(n-\alpha)^3$. Classically speaking at these high laser frequencies it is only in a region close to the nucleus that the acceleration of a Rydberg electron is sufficiently large that an appreciable energy exchange of the order of $\Delta\epsilon \approx \omega$ can take place between the laser field and the Rydberg electron (compare also with Eq.(5)). As a consequence the interaction of a Rydberg electron with a laser field of moderate intensity and sufficiently high frequency is completely different from its interaction with a microwave field whose frequency is comparable with its classical Kepler frequency $1/T_n$. Even if the field strength of such a microwave field is small in the sense that $\alpha_{osc} \ll 1$, the small frequency of the microwave field implies that energy can be exchanged with the microwave field essentially at any distance of the Rydberg electron from the atomic nucleus.

(2) *The Coulomb region:*$(O(1) < r < a)$

Outside the core region the dynamics of a highly excited Rydberg electron is dominated by the $1/r$ Coulomb potential of the positively charged ionic core. If the Rydberg electron is influenced by a weak external electric or magnetic field this is only valid for distances of the Rydberg electron from the nucleus which are smaller than the critical distance $a \gg 1$ at which the external potentials are no longer negligible. If this critical distance is located inside the classically accessible region, i.e. $a < 1/\mid \epsilon_n \mid$, these external fields influence the dynamics of the Rydberg electron significantly.

(3) *The asymptotic region:* $(1 \ll a < r)$

In the asymptotic region the influence of weak external fields is as important as the Coulomb force originating from the positively charged ionic core. In general, in this region the resulting dynamics of the Rydberg electron is complicated by the fact that its classical dynamics is no longer integrable and exhibits

signatures of chaos.

In each of these characteristic spatial regimes different approximations can be applied for the dynamical description of the Rydberg electron. All photon absorption and emission processes and all electron correlation effects which take place inside the core region have to be described quantum mechanically. As the Bohr radius is small in comparison with the extension of the Coulomb region and of the asymptotic region, outside the core region the dynamics of a Rydberg electron can be described with the help of semiclassical methods.

Starting from these elementary considerations a systematic theoretical description of Rydberg electrons can be developed which is based on a synthesis of semiclassical methods and of concepts of quantum defect theory (Alber 1989, Alber and Zoller 1991). Thereby solutions of the Schrödinger equation which are valid inside the core region and at the boundary to the Coulomb region have to be matched to semiclassical wave functions which are valid in the Coulomb region and in the asymptotic region. The values of the wave function at the border between the core region and the Coulomb region are determined by the solution of the Schrödinger equation inside the core region. Within the framework of quantum defect theory these values are determined by approximately energy independent quantum defect parameters. These quantum defect parameters originate from two different types of interactions, namely electron correlation effects and laser-induced photon absorption and emission processes. For moderate laser intensities and sufficiently high frequencies these latter type of processes give rise to intensity dependent quantum defects. Thus, in the simplest case of a one-channel approximation, for example, these interactions inside the core region can be characterized by a complex quantum defect of the form (Alber and Zoller 1988)

$$\mu = \alpha + i\beta. \tag{3}$$

The real part of this quantum defect defines the energies of the Rydberg electron in the absence of the laser field, i.e. $\epsilon_n = -1/[2(n-\alpha)^2]$. The imaginary part β describes the influence of laser-induced transitions of the Rydberg electron into continuum states well above threshold. In lowest order of perturbation theory it is given by

$$\beta = \pi \mid \langle \epsilon = \omega \mid \mathbf{d} \cdot \mathbf{E}_0 \mid \epsilon = 0 \rangle \mid^2 \tag{4}$$

with $\mathbf{d}$ denoting the atomic dipole operator. For hydrogen and linearly polarized laser light, for example, this imaginary part of the quantum defect can be evaluated approximately with the help of the Bohr correspondence principle. According to this principle the dipole matrix element entering Eq.(4) is approximated by a Fourier coefficient of the classical trajectory of a Rydberg electron

of energy $\epsilon = 0$ (Landau and Lifshitz 1975), i.e.

$$\langle \epsilon = \omega \mid \mathbf{d} \cdot \mathbf{E}_0 \mid \epsilon = 0 \rangle = \frac{1}{2\pi} \int_{-\infty}^{\infty} dt e^{i\omega t} \mathbf{x}(t) \cdot \mathbf{E}_0 = \frac{6^{2/3}}{2\pi\sqrt{3}} \Gamma(2/3) \omega^{-5/3} \mid \mathbf{E}_0 \mid . \tag{5}$$

($\Gamma(x) = \int_0^\infty du u^{x-1} e^{-u}$ denotes the Euler gamma function.) Thereby $\mathbf{x}(t)$ describes the parabolic classical trajectory of an electron which moves in the Coulomb field of the nucleus with energy $\epsilon = 0$. Consistent with the previous qualitative discussion the $\omega^{-5/3}$-dependence in Eq.(5) demonstrates that the dominant contribution to this dipole matrix element originates from a spatial region around the nucleus with a size of the order of $r_c \approx \omega^{-2/3}$. This characteristic size r_c is the distance a classical electron of (asymptotic) energy $\epsilon = 0$ can depart from the nucleus during the relevant photon absorption time $t_{photon} \approx 1/\omega$.

In the Coulomb and asymptotic region the quantum mechanical state can be determined semi classically. In order to make these ideas more precise let us consider the general form of the semiclassical solution of the time independent Schrödinger equation which is valid in the Coulomb and asymptotic region. It has the general form (Maslov and Fedoriuk 1981, Delos 1986)

$$\psi(\epsilon, \mathbf{x}) \quad = \quad \sum_j \varphi(\epsilon, \mathbf{y}_j) \sqrt{\frac{J(0, \mathbf{y}_j)}{\mid J(t_j, \mathbf{y}_j) \mid}} e^{i[S_j(t_j, \mathbf{y}_j) - \mu_j(t_j)\pi/2]}. \tag{6}$$

This wave function is determined by two different types of quantities, namely the probability amplitude $\varphi(\epsilon, \mathbf{y})$ of finding the electron at position $\mathbf{y}$ on the boundary between the core region and the Coulomb region and by quantities which describe the classical motion of the Rydberg electron outside the core region (compare with Fig. 1). The probability amplitude $\varphi(\epsilon, \mathbf{y})$ is determined by the quantum defect parameters which describe the electron correlations and the electron-laser interaction inside the core region. According to Eq.(6) the probability amplitude $\psi(\epsilon, \mathbf{x})$ of finding the electron at position $\mathbf{x}$ outside the core region is also determined by properties of all those classical trajectories j which start at the boundary between the core region and the Coulomb region at position $\mathbf{y}$ and reach the final point $\mathbf{x}$ at any 'time' t. In this context the variable t represents a curve parameter and not a physical time. Together with the initial positions $\mathbf{y}$ the curve parameter t constitutes a global coordinate system for the family of classical trajectories which leave the core region and which form a Lagrangian manifold (Maslov and Fedoriuk 1981, Delos 1986). The important classical properties of trajectory j which determine $\psi(\epsilon, \mathbf{x})$ are:

1. its classical action (eikonal) $S_j(t_j, \mathbf{y}_j)$,

2. the determinant of its Jacobi field

$$J(t_j, \mathbf{y}_j) = \frac{dx_1 \wedge dx_2 \wedge dx_3}{dt \wedge dy_1 \wedge dy_2} \mid_j$$

which characterizes its stability properties, and

3. its Maslov index $\mu_j(t_j)$ which characterizes the number of conjugate points and their multiplicity.

According to this general theoretical approach it is apparent that Rydberg systems differ from one another only as far as their dynamics inside the core region is concerned. This part of the dynamics can be described generally by a few quantum defect parameters. Thus Rydberg systems exhibit universal behavior and the quantum defect parameters characterize the associated universality classes. Furthermore, the semiclassical analysis of the dynamics of the Rydberg electron in the Coulomb region and in the asymptotic region implies that probability amplitudes describing atomic transitions between an initial and a final state can be represented as a sum of contributions which are associated with all possible classical paths (including their multiple returns) which connect the regions of support of the initial and the final state. In particular, if the dominant contribution of a transition amplitude originates from the core region, for example, it is all classical paths which start and end inside the core region which are relevant for the theoretical description. On the basis of this combination of methods of quantum defect theory with semiclassical path representations for relevant quantum mechanical transition amplitudes many aspects of the coherent dynamics of electronic Rydberg wave packets have already been described successfully (Beims and Alber 1993, 1996, Alber et al. 1994, Zobay and Alber 1998).

2 Dissipative dynamics of electronic Rydberg wave packets

So far in the context of wave packet dynamics of material particles the investigation of dissipative and stochastic influences which destroy quantum coherence has not received much attention. Definitely, to some extent this may be attributed to the complications arising from the high level densities which have to be taken into account for a proper theoretical description of wave packet dynamics. In general they turn the solution of master equations for the relevant density operator into a difficult mathematical and numerical problem. Electronic wave packets in Rydberg systems are an extreme example of this kind due to their almost macroscopic size and the infinitely high level density of Rydberg states at an ionization threshold. In the subsequent discussion it will be demonstrated that a combination of the semiclassical methods discussed in Sec. 1 together with stochastic simulation methods constitutes a powerful theoretical approach for describing many aspects of the destruction of quantum coherence in wave packet dynamics. In addition, this theoretical approach offers insight into the intricate interplay between the semiclassical aspects of the dynamics of

a Rydberg electron outside the core region and its coupling to the radiation field inside the core region. In the subsequent sections two types of physical processes will be discussed in detail by which this coupling to the radiation field can destroy the quantum coherence of an electronic wave packet, namely spontaneous emission of photons and the intrinsic fluctuations of a laser field. Motivated by the recent interest in laser-induced two-electron excitation processes, in Sec. 2.1 characteristic effects of radiative damping are explored which are mediated by the correlation between an electronic Rydberg wave packet and a resonantly excited, tightly bound core electron. In Sec. 2.2 it is demonstrated that as a result of the peculiar threshold properties of Rydberg systems the destruction of quantum coherence which is brought about by a fluctuating laser field gives rise to a variety of novel phenomena.

2.1 Radiative damping mediated by electron correlations

Due to the long radiative life times of Rydberg states (radiative life times scale as $(n-\alpha)^3$ (Gallagher 1994)) the direct influence of spontaneously emitted photons is negligible under typical laboratory situations. However, destruction of quantum coherence originating from radiative damping might become significant in cases in which more than one atomic or molecular electron is excited resonantly by a laser field. In such cases the influence of a photon which is emitted spontaneously by one of these excited electrons can influence another excited Rydberg electron via electron correlation effects. Isolated core excitation (ICE) processes (Cooke et al. 1978) are a particular class of laser-induced two-electron excitation processes which has received considerable attention recently. In the following it is demonstrated that in these types of excitation processes the dissipative influence of radiative damping mediated by electron correlations may influence the dynamics of electronic wave packets significantly.

ICE excitation processes have been studied extensively in the alkaline earth elements as the corresponding singly-charged ions are excited easily with laser fields in the optical or near-uv regime. In Fig. 2 a typical laser-induced ICE process is shown schematically for a magnesium atom. In a first step, the atom is excited from its $|3s^2\rangle$ ground state to a Rydberg state $|3snd\rangle$ by two-photon excitation. After this excitation process the atom consists of the Mg^+(3s) ionic core and the nd-Rydberg electron which tends to be located at large distances from the core. By applying a second laser pulse tuned to a resonance of the Mg^+ ion the remaining core electron is excited, e.g. to the $3p$-state of the ionic core. The direct influence of the laser field on the highly excited Rydberg electron is usually negligible in comparison to its interaction with the second, tightly bound valence electron. But the laser field influences the Rydberg electron indirectly by electron correlation effects. Immediately after the core transition the Rydberg electron experiences a "shakeup" by the different short-range core potential to which it has to accommodate. A quantitative measure for the degree of this shakeup is given by the difference between the quantum defects of

the two channels associated with the $3s$ and the $3p$-states of the ionic core. The early work on ICE spectroscopy of alkaline earth elements has concentrated on non-resonant core transitions which can be described in lowest order of perturbation theory with respect to the laser field (Gallagher 1994). Non-perturbative effects of laser fields have become of interest only recently in connection with the development of powerful tunable laser sources (Jones and Bucksbaum 1991, Stapelfeldt et al. 1991, Robicheaux 1993, Grobe and Eberly 1993). They are particularly important in resonant core excitation processes in which one of the laser fields induces Rabi oscillations of the ionic core. A variety of new coherent effects have been predicted theoretically in this context (Robicheaux 1993, Hanson and Lambropoulos 1995, Zobay and Alber 1995, van Druten and Muller 1995) which rely on the coherent interplay between the Rabi oscillations of the ionic core and the dynamics of an electronic Rydberg wave packet which is influenced by these Rabi oscillations through the resulting shakeup processes (For a review on these theoretical developments see Zobay and Alber 1998). However, due to the possibility of spontaneous emission of photons by the resonantly excited core electron all these effects are expected to be particularly sensitive to the resulting destruction of quantum coherence.

In order to investigate these dissipative effects in detail let us consider a typical laser-induced two-electron excitation process in an alkaline earth atom as represented in Fig. 3. It is assumed that the atom is prepared initially in its ground state $|g\rangle$. The atom is situated in a cw-laser field whose electric field strength is given by $\mathbf{E}(t) = \mathcal{E}\mathbf{e}e^{-i\omega t} + c.c.$ and which is tuned near resonance with a transition of the positively charged ionic core. Typically electron correlations imply that as long as the atom remains in its initial state $|g\rangle$ this laser field is well detuned from any atomic transition. Thus the laser field has negligible effect on the atomic dynamics. But as soon as an outer valence electron is excited to Rydberg state close to an ionization threshold the cw-laser field starts to induce transitions between the two resonantly coupled states of the ionic core which have energies ϵ_1 and ϵ_2, respectively. Let us concentrate on a case in which one of the valence electrons is excited coherently to Rydberg states by a short and weak laser pulse with electric field strength $\mathbf{E}_a(t) = \mathcal{E}_a(t)\mathbf{e}_a e^{-i\omega_a t} + c.c.$ (Typically the pulse envelope $\mathcal{E}_a(t)$ will be modeled by a Gaussian shape centered around time t_a with pulse duration τ_a). Thus a radial electronic Rydberg wave packet is prepared by this short laser pulse (Alber and Zoller 1991). This wave packet moves in the Coulomb field of the positively charged ionic core. Whenever it penetrates the core region it is shaken up by the Rabi oscillations of the resonantly driven core. Furthermore, whenever the core emits a photon spontaneously this emission process will disrupt the relative phases of the electronic wave packet and will thus destroy quantum coherence. The dynamics of this electronic wave packet under the influence of the Rabi oscillations of the ionic core can be investigated by typical pump-probe experiments, for example.

For the theoretical description of the resulting destruction of quantum coherence one has to solve the corresponding optical Bloch equation for the density

operator of the two atomic valence electrons. In the case depicted in Fig. 3, for example, the optical Bloch equation is given by (Zobay and Alber 1996)

$$\dot{\rho}(t) = -i[H, \rho(t)] + \frac{1}{2}\{[L, \rho(t)L^{\dagger}] + [L\rho(t), L^{\dagger}]\}. \tag{7}$$

Thereby the Hamiltonian

$$H \quad = \quad \sum_{i,j=1,..,3} H_{i,j} + V_{ICE} \tag{8}$$

characterizes the coherent part of the dynamics. The dynamics of the valence electrons is described by the Hamiltonian

$$H_{i,j} = (\mathbf{h}_{jj}\delta_{ij} + \mathbf{V}_{ij} + \epsilon_{cj}\delta_{ij})|\Phi_i\rangle\langle\Phi_j| \tag{9}$$

with

$$\mathbf{h}_{jj} = -\frac{1}{2}\frac{d^2}{dr^2} + \frac{l_j(l_j+1)}{2r^2} - \frac{1}{r}. \tag{10}$$

The short-range potential $\mathbf{V}_{ij}$ describes electron-correlation effects originating from the residual core electrons (Aymar et al. 1996). In ICE transitions the angular momentum l of the excited Rydberg electron is conserved to a good degree of approximation, i.e. $l_1 = l_2 = l$ (Gallagher 1994). In the rotating wave approximation the channel thresholds ϵ_{cj} are given by $\epsilon_{c1} = \epsilon_1$, $\epsilon_{c2} = \epsilon_2 - \omega$, $\epsilon_{c3} = \epsilon_3 - \omega$. The operator

$$V_{ICE} = -\frac{1}{2}\Omega(|\Phi_2\rangle\langle\Phi_1| + |\Phi_1\rangle\langle\Phi_2|) \otimes \mathbf{1}_r \tag{11}$$

describes the laser-induced core transitions between the core states $|\ \Phi_1\rangle$ and $|\ \Phi_2\rangle$ and Ω is the Rabi frequency originating from the cw-laser field. The operator $\mathbf{1}_r$ denotes the identity operator for the radial coordinate of the Rydberg electron. Thus the role of the Rydberg electron as a spectator becomes obvious from Eq.(11).

The stochastic part of the dynamics of the density operator $\rho(t)$ is described by the Lindblad operator

$$L = \sqrt{\kappa}|\Phi_1\rangle\langle\Phi_2| \otimes \mathbf{1}_r \tag{12}$$

which characterizes the radiative decay of the ionic core from its excited state to its ground state by spontaneous emission of photons with rate κ.

Due to the high level density of Rydberg states close to an ionization threshold and due to the presence of the adjacent electron continuum usually severe problems arise, if one tries to solve the optical Bloch equation (7) numerically by expanding the density operator $\rho(t)$ into a basis set of atomic energy eigenfunctions. Many of these problems can be circumvented successfully by combining the semiclassical methods as discussed in Sec. 1 with stochastic simulation

methods (Zobay and Alber 1996). Besides numerical advantages this approach gives also direct insight into the classical aspects of the dynamics of the Rydberg electron and the destruction of quantum coherence caused by the radiative decay of the core. Thereby the density operator is represented by a (fictitious) ensemble of pure states which are associated with definite numbers of spontaneously emitted photons (Mollow 1975), i.e.

$$\rho(t) = \sum_{N=0}^{\infty} \rho^{(N)}(t), \tag{13}$$

with the N-photon contributions

$$\rho^{(N)}(t) = \int_0^t dt_N \int_0^{t_N} dt_{N-1} \cdots \int_0^{t_2} dt_1 |\psi(t|t_N, ..., t_1)\rangle\langle\psi(t|t_N, ..., t_1)|.$$

The time evolution of the N-photon states $|\psi(t|t_N, ..., t_1)\rangle$ is given by

$$\begin{aligned} |\psi(t|t_N, ..., t_1)\rangle &= e^{-iH_{\rm eff}(t-t_N)}\Theta(t-t_N)Le^{-iH_{\rm eff}(t_N-t_{N-1})}\Theta(t_N-t_{N-1})L\cdots \\ &\quad Le^{-iH_{\rm eff}t_1}\Theta(t_1)|\psi(t=0)\rangle \end{aligned} \tag{14}$$

with the effective (non-Hermitian) Hamiltonian

$$H_{\rm eff} = H - \frac{i}{2}L^\dagger L. \tag{15}$$

($\Theta(x)$ is the unit step function.) The physical interpretation of Eq.(14) is straight forward. With each emission of a photon at one of the N random emission times $t_1 \le t_2 \le ... \le t_N$ the quantum state 'jumps' into a new state by application of the Lindblad operator of Eq.(12). Between two successive jumps the state evolves according to the Hamiltonian of Eq.(15). Thus the decomposition of Eq.(13) may also be interpreted as an unraveling of the density operator into contributions associated with all possible quantum jumps. This decomposition of the density operator $\rho(t)$ offers significant advantages in cases in which the number of spontaneously emitted photons is small or in which the evaluation of the relevant pure states can be simplified by the application of semiclassical methods. In particular, it is possible to derive general semiclassical path representations for the N-photon states of the optical Bloch equation (7). Thus all physical observables of interest can be expressed as a sum of probability amplitudes which are associated with repeated returns of a Rydberg electron to the ionic core. During its motion under the influence of the Coulomb potential of the ionic core photons may be emitted spontaneously by the laser-excited core at any position of the Rydberg electron along its path. These photon emission processes disrupt the coherent quantum mechanical time evolution of the Rydberg electron.

As an example, let us consider a coherent process which has received considerable attention recently, namely laser-induced stabilization against autoionization (Hanson and Lambropoulos 1995). This effect is based on a synchronization

between the dynamics of the ionic core, which performs Rabi oscillations, and the dynamics of a laser-prepared electronic wave packet. This effect may be understood as follows: At the time of the preparation of the electronic Rydberg wave packet by the short laser pulse the core is in its ground state. If the mean Kepler period $T_{orb} = 2\pi(-2\overline{\epsilon})^{-3/2}$ ($\overline{\epsilon}$ is the mean excited energy of the Rydberg electron) of this wave packet is chosen equal to a multiple of the Rabi period $T_{Rabi} = 2\pi/\Omega$ of the core, the Rydberg electron will encounter the core in the ground state at each of its subsequent returns to the nucleus. As autoionization of a Rydberg electron can take place only inside the core region (Seaton 1983, Fano and Rau 1986, Aymar et al 1996), this implies that the effective autoionization rate of the electronic wave packet will become much smaller than the autoionization rate of the mean excited Rydberg state $\Gamma_{\overline{n}}$ in the absence of the laser field. In addition, it has been demonstrated (Hanson and Lambropoulos 1995) that this suppression of autoionization is also accompanied by a reduction of dispersion of the electronic wave packet. This suppression of dispersion is brought about by the Rabi-oscillating core which acts like a quantum-mechanical shutter and effectively cuts off the tails of the wave packet which arrive at the nucleus out of phase with small probability. As this stabilization against autoionization is based on the coherent interplay between electron correlations and laser-induced Rabi oscillations it is expected to be particularly sensitive against the destruction of quantum coherence due to spontaneous emission of photons by the ionic core.

In the presence of radiative decay of the ionic core the physical picture is changed significantly. In the simplest case of synchronization, i.e. for $T_{orb} = T_{Rabi}$, the first photon will be emitted spontaneously by the ionic core most probably at a time $(M + 1/2)T_{Rabi}$ (with M denoting any integer) because then the core is in its excited state with high probability. Due to the synchronization at these times the electronic Rydberg wave packet is close to the outer turning point of its Kepler orbit. The spontaneous emission of a photon reduces the excited core to its ground state. Therefore, at the subsequent return of the electronic wave packet to the core at time $(M + 1)T_{orb}$ the ionic core will be in its excited state so that the Rydberg electron will autoionize on a time scale of the order of $1/\Gamma_{\overline{n}}$. Thus, the laser-induced stabilization against autoionization will be destroyed. Typically, $\Gamma_{\overline{n}} \gg \kappa$ so that the Rydberg electron will autoionize with high probability long before the core can emit a second photon spontaneously. Consequently, it is expected that the influence of the radiative damping on this coherent stabilization phenomenon can be described approximately by taking into account only the zero-and one-photon contributions of the density operator $\rho(t)$.

The influence of radiative damping described above manifests itself clearly in the time-dependent autoionization rate $\gamma(t)$ into channel three, for example, which results from the dynamics of the electronic Rydberg wave packet. An experimental technique for measuring $\gamma(t)$ has been developed recently (Lankhuijzen and Noordam 1996). This time-dependent ionization rate $\gamma(t)$ can be

decomposed into N-photon contributions with the help of semiclassical path representations, i.e.

$$\gamma(t) = \sum_{N=0}^{\infty} \int_0^t dt_N \cdots \int_0^{t_2} dt_1 \gamma^{(N)}(t). \tag{16}$$

It is expected that the zero- and one-photon contributions (Zobay and Alber 1996)

$$\begin{aligned}
\gamma^{(0)}(t) &= \frac{1}{2\pi}(1 - e^{-4\pi \mathrm{Im}\mu_2}) \mid \int_{-\infty+i0}^{\infty+i0} d\epsilon_1 e^{-i\epsilon_1 t}(0,1,0)\mathbf{O} \sum_{M_1=0}^{\infty} (e^{i2\pi\bar{\nu}_1}\tilde{\chi})^{M_1} \times \\
&\quad e^{i2\pi\bar{\nu}_1}\tilde{\mathcal{D}}^{(-)}_{g\mathbf{e}_a}\tilde{\mathcal{E}}_a(\epsilon_1 - \epsilon) \mid^2, \\
\gamma^{(1)}(t) &= (\frac{1}{2\pi})^3(1 - e^{-4\pi \mathrm{Im}\mu_2}) \mid \int_{-\infty+i0}^{\infty+i0} d\epsilon_1 d\epsilon_2 e^{-i\epsilon_2(t-t_1)} e^{-i\epsilon_1 t_1}(0,1,0)\mathbf{O} \times \\
&\quad \sum_{M_2=0}^{\infty} (e^{i2\pi\bar{\nu}_2}\tilde{\chi})^{M_2} \tilde{\mathbf{S}}^{(M_2,M_1)}_{2,1} \sum_{M_1=0}^{\infty} (\tilde{\chi} e^{i2\pi\bar{\nu}_1})^{M_1} \tilde{\mathcal{D}}^{(-)}_{g\mathbf{e}_a}\tilde{\mathcal{E}}_a(\epsilon_1 - \epsilon) \mid^2
\end{aligned} \tag{17}$$

are dominant. In Eqs.(17) the laser-induced excitation by the short laser pulse is characterized by the Fourier transform of the pulse envelope

$$\tilde{\mathcal{E}}_a(\Delta\epsilon) = \int_{-\infty}^{\infty} dt \mathcal{E}_a(t) e^{i\Delta\epsilon(t-t_a)} \tag{18}$$

and by the (3×1)-column vector $\tilde{\mathcal{D}}^{(-)}_{g\mathbf{e}_a}$ whose components are the energy normalized photoionization dipole matrix elements (Seaton 1983) into channels one, two and three. The dynamics of the Rydberg electron under the influence of the Rabi oscillations of the ionic core are described by the (3×3) scattering matrix $\tilde{\chi}$ and by the (3×3) diagonal matrix $e^{i2\pi\bar{\nu}}$ with matrix elements $(e^{i2\pi\bar{\nu}})_{jj} = e^{2i\pi[2(\bar{\epsilon}_{cj}-\epsilon)]^{-1/2}}\Theta(\tilde{\epsilon}_{cj} - \epsilon)$ $(j = 1, 2, 3)$. All matrices and column vectors with a tilde refer to the basis of photon-dressed core states $|\tilde{\Phi}_j\rangle$ $(j = 1, 2, 3)$ (Robicheaux 1993, Zobay and Alber 1995). These dressed channel states are related to the corresponding bare states $|\Phi_j\rangle$ by the orthogonal transformation $\mathbf{O}$ which diagonalizes the laser-induced core coupling, i.e.

$$\mathbf{O}^T[\epsilon_c - i\kappa/2|\Phi_2\rangle\langle\Phi_2| - \frac{1}{2}\Omega(|\Phi_2\rangle\langle\Phi_1| + |\Phi_1\rangle\langle\Phi_2|)]\mathbf{O} = \tilde{\epsilon}_c. \tag{19}$$

Thereby the diagonal matrix $\tilde{\epsilon}_c$ (ϵ_c) contains the energies of the dressed (bare) core states. Thus the relations $\tilde{\mathcal{D}}^{(-)}_{g\mathbf{e}_a} = \mathbf{O}^T\mathcal{D}^{(-)}_{\mathbf{ge_a}}$ and $\tilde{\chi} = \mathbf{O}^T\chi\mathbf{O}$ hold with the bare photoionization dipole matrix elements $\mathcal{D}^{(-)}_{\mathbf{ge_a}}$ and with the bare scattering matrix

$$\boldsymbol{\chi} = \begin{pmatrix} e^{2\pi i\mu_1} & 0 & 0 \\ 0 & e^{2\pi i\mu_2} & \chi_{23} \\ 0 & \chi_{32} & \chi_{33} \end{pmatrix}. \tag{20}$$

The quantum defects of the bare channels one and two are denoted μ_j. These channels have opposite parity and cannot be coupled by electron correlation effects. The matrix elements χ_{23} and χ_{32} characterize the configuration interaction between channels 2 and 3 which results in autoionization of channel 2. The autoionization rate of a Rydberg state of channel 2 with principal quantum number n is related to the imaginary part of the quantum defect μ_2 by $\Gamma_n = 2\mathrm{Im}(\mu_2)/[n - \mathrm{Re}(\mu_2)]^3$.

Eqs.(17) are examples of semiclassical path representations for the zero- and one-photon ionization rates $\gamma^{(0)}(t)$ and $\gamma^{(1)}(t)$. Their physical interpretation is straight forward: After the initial excitation by the short laser pulse those fractions of the electronic Rydberg wave packet which are excited into closed photon-dressed core channels return to the core region periodically. The integers M_1 and M_2 count the numbers of these returns. Between two successive returns the Rydberg electron acquires a phase of magnitude $(2\pi\tilde{\nu})_{jj}$ while moving in the photon-dressed core channel j. This phase equals the classical action of motion along a purely radial Kepler orbit with zero angular momentum and energy $\epsilon - \tilde{\epsilon}_{cj} < 0$. Entering the core region the Rydberg electron is scattered into other photon-dressed core channels by laser-modified electron correlation effects which are described by the scattering matrix $\tilde{\chi}$. The ionic core can emit a photon spontaneously at any time during the motion of the Rydberg electron. Quantitatively this photon emission process is described the the quantity

$$\tilde{\mathbf{S}}_{2,1}^{(M_2,M_1)} = \int_0^{T_{M_1,M_2}} d\tau e^{2i\pi\bar{\nu}_2(1-\tau/T_{M_1,M_2})}(e^{-i\pi/2}\tilde{\mathbf{L}})e^{2i\pi\bar{\nu}_1\tau/T_{M_1,M_2}} \qquad (21)$$

in Eqs.(17) with $T_{M_1,M_2} = t/(M_1 + M_2 + 1)$. According to Eq.(21) this spontaneous photon emission by the ionic core can take place at any time τ between two successive returns of the Rydberg electron to the core region. At time τ the Rydberg electron has acquired a phase of magnitude $(2\pi\tilde{\nu})_{jj}\tau/T_{M_1,M_2}$ in channel j. The disruption of the phase of the Rydberg electron by this spontaneous emission process is described by the action of the Lindblad operator $\tilde{\mathbf{L}} = \mathbf{O}^T\mathbf{L}\mathbf{O}$. It also leads to a phase change of magnitude $(\pi/2)$. After the completion of the photon emission process the Rydberg electron acquires an additional phase of magnitude $(2\pi\tilde{\nu})_{jj}(1 - \tau/T_{M_1,M_2})$ in the photon-dressed core channel j until it reaches the core region again.

A representative time evolution of the autoionization rate $\gamma(t)$ is shown in Fig. 4. The full curve in Fig. 4a has been obtained by numerical solution of the optical Bloch equation (7) with the help of a conventional basis expansion in atomic energy eigenstates. The corresponding zero- and one-photon contributions are also presented in Figs. 4b and 4c. In Fig. 4 the sum of zero- and one-photon contributions are not plotted as they are indistinguishable from the numerical result (full curve in Fig.4a). The chosen parameters represent typical values realizable in alkaline earth experiments. The comparison of $\gamma(t)$ (full curve of Fig.4a) with the corresponding result in the absence of radiative

damping (dotted curve in Fig.4a) demonstrates that the influence of radiative damping is already significant at interaction times of the order of T_{orb}. With the help of the zero- and one-photon contributions of Eq.(17) the dissipative influence of radiative damping can be analyzed in detail. As apparent from Fig. 4b, the zero-photon rate vanishes at integer multiples of the mean Kepler period T_{orb} because at these times the core is in its ground state. The maxima of Fig. 4b at times $(M + 1/2)T_{orb}$ originate from fractions of the electronic wave packet which are close to the core at times when the core is in its excited state. Also visible are typical revival effects at times of the order of $25T_{orb}$. The one-photon rate of Fig. 4c exhibits maxima and minima at times MT_{orb} and $(M + 1/2)T_{orb}$. These maxima indicate that the photon is emitted by the ionic core most probably whenever the Rydberg electron is close to the outer turning point of its classical Kepler orbit. Thus, the core will be in its excited state when the Rydberg electron returns to the nucleus so that autoionization will take place with a high probability.

2.2 Electronic wave packets in fluctuating laser fields

The main aim of this section is to discuss characteristic effects which govern the dynamics of a Rydberg electron in an intense and fluctuating laser field. It is demonstrated that for moderate laser intensities (compare with Sec. 1 Eq.(2)) a variety of novel, non-perturbative effects appear which influence the long time behavior of Rydberg electrons significantly. A generic consequence of the interplay between the peculiar threshold phenomena of Rydberg systems and the destruction of quantum coherence due to laser fluctuations is stochastic ionization (Alber and Eggers 1997). It is demonstrated that this process also implies an upper time limit on the applicability of two-level approximations even in cases in which all characteristic frequencies, i.e. Rabi frequencies and laser bandwidths, are small in comparison with the Kepler frequency of a resonantly excited Rydberg electron.

Nowadays laser fluctuations can be controlled to such a degree that it is possible to realize various theoretical models of laser radiation in the laboratory (Vemuri et al. 1991). One of the most elementary theoretical models of laser radiation is the phase diffusion model (PDM) (Haken 1970). It describes approximately the electric field produced by an ideal single mode laser which is operated well above the laser threshold. Thereby the electric field of a laser is represented by a classical, stochastic process with well stabilized amplitude and a fluctuating phase, i.e.

$$\mathbf{E}(t) = \mathbf{E}_0 e^{i\Phi(t)} e^{-i\omega t} + c.c. \; . \tag{22}$$

The fluctuations of the phase $\Phi(t)$ are modeled by a real-valued Wiener process (Klöden and Platen 1992), i.e.

$$M\, d\Phi(t) = 0, [d\Phi(t)]^2 = 2b dt \tag{23}$$

Thereby M indicates the mean over the statistical ensemble. The PDM implies a Lorentzian spectrum of the laser radiation with bandwidth b.

In order to investigate the influence of laser fluctuations on the optical excitation of Rydberg states close to an ionization threshold let us consider the simplest possible case, namely one-photon excitation from a tightly bound initial state $|g\rangle$ with energy ϵ_g. In the dipole and rotating wave approximation the Hamiltonian which describes this excitation process is given by

$$\begin{aligned} H(\Phi(t)) &= \epsilon_g|g\rangle\langle g| + \sum_n \epsilon_n|n\rangle\langle n| - \\ &\quad \sum_n (|n\rangle\langle g|\langle n|\mathbf{d}|g\rangle \cdot \mathbf{E}_0 e^{i\Phi(t)} e^{-i\omega t} + \text{h.c.}). \end{aligned} \tag{24}$$

In Eq.(24) the index n refers to Rydberg and continuum states. The energies of the excited Rydberg states are denoted ϵ_n and $\mathbf{d}$ is the atomic dipole operator. Let us assume for the sake of simplicity that the excited Rydberg and continuum states can be described with the help of quantum defect theory in a one channel approximation (Seaton 1983). Thus they are characterized by an approximately energy independent quantum defect $\mu = \alpha + i\beta$. As has been explained in Sec. 1 (Eq.(4)) the imaginary part β describes photon absorption from the highly excited Rydberg states to continuum states well above threshold.

For the description of non-perturbative aspects of this laser excitation process one has to solve the time dependent Schrödinger equation with the stochastic Hamiltonian (24) (interpreted as a stochastic differential equation of the Ito type (Klöden and Platen 1992)) together with the stochastic differential equation for the phase (23). It is the simultaneous presence of the Coulomb threshold with its infinitely many bound states and the continuum on the one hand and the laser fluctuations on the other hand which makes this solution a highly nontrivial task. Nevertheless, for the case of the PDM the resulting mathematical and numerical problems can be circumvented successfully (Alber and Eggers 1997). Thus even analytical results can be derived in the limit of long interaction times which is dominated by stochastic ionization of the Rydberg electron. Thus, let us start from the equation of motion for the mean values $\rho_{nn'}(t) = M\langle n \mid \psi(t)\rangle\langle\psi(t) \mid n'\rangle$, $\rho_{ng}(t) = [\rho_{gn}(t)]^* = Me^{-i\Phi(t)}\langle n \mid \psi(t)\rangle\langle\psi(t) \mid g\rangle$ and $\rho_{gg}(t) = M \mid \langle g \mid \psi(t)\rangle \mid^2$ which can be combined to form a density operator $\rho(t)$ (Agarwal 1976). From Eqs. (23) and (24) it can be shown that this density operator fulfills the master equation

$$\frac{d}{dt}\rho(t) = -i[H_{mod}, \rho(t)] + \frac{1}{2}\{[L, \rho(t)L^\dagger] + [L\rho(t), L^\dagger]\}. \tag{25}$$

Thereby the modified Hamiltonian $H_{mod} \equiv H(\Phi(t) \equiv 0)$ describes laser induced excitation of Rydberg states close to threshold in the absence of phase fluctuations. The destruction of quantum coherence which is brought about by the laser fluctuations is characterized by the Lindblad operator

$$L = \sqrt{2b}|g\rangle\langle g|. \tag{26}$$

On the basis of this master equation Fourier representations can be developed for the density matrix elements whose kernels can be determined explicitly with the help of quantum defect theory. Thus all complications arising from the Coulomb threshold are taken into account properly. These Fourier representations are useful for numerical calculations of averaged transition probabilities which are highly accurate even in the limit of long interaction times. Furthermore, these representations are convenient starting points for the derivation of analytical results. Thus, the averaged initial state probability $\rho_{gg}(t)$, for example, is given by (Alber and Eggers 1997)

$$\begin{aligned}\rho_{gg}(t) &= \sum_{N=0}^{\infty}\frac{1}{2\pi}\int_{-\infty+i0}^{\infty+i0}dz e^{-izt}A_{gg}(z)[2bA_{gg}(z)]^N = \\ &\frac{1}{2\pi}\int_{-\infty+i0}^{\infty+i0}dz e^{-izt}A_{gg}(z)[1-2bA_{gg}(z)]^{-1} \end{aligned} \tag{27}$$

with

$$\begin{aligned}A_{gg}(z) &= U(z)+U^*(-z), \\ U(z) &= \{-C_1(z)+C_2(z)+ \\ &i\sum_{\mathrm{Re}\tilde{\epsilon}_n<0}[1-\frac{d}{dz}\Sigma^*(z_1-z)]^{-1}[z_1-\overline{\epsilon}+ib-\Sigma(z_1)]^{-1}\mid_{z_1=z+\tilde{\epsilon}_n^*}\}\Theta(z)\end{aligned} \tag{28}$$

and with

$$\begin{aligned}C_1(z) &= \frac{1}{2\pi(z+2ib)}\ln\frac{z-\overline{\epsilon}+i(b+\gamma/2)}{-\overline{\epsilon}+i(\gamma/2-b)}, \\ C_2(z) &= \frac{1}{2\pi[z+i(\gamma+2b)]}\ln\frac{z-\overline{\epsilon}+i(b+\gamma/2)}{-\overline{\epsilon}+i(\gamma/2+b)}.\end{aligned} \tag{29}$$

In the spirit of the discussion of Sec. 2.1. (compare with Eq.(13)) $\rho_{gg}(t)$ is represented as a sum of contributions of all possible quantum jumps N which can be induced by the Lindblad operator of Eq.(26). According to Eq.(27) these contributions give rise to a geometric series which can be summed easily. The sum appearing in Eq.(28) extends over all dressed states $\tilde{\epsilon}_n$ of the effective Hamiltonian $H_{\mathrm{eff}} = H_{mod} - iL^\dagger L/2$. The mean excited energy is given by $\overline{\epsilon} = \epsilon_g + \omega + \delta\omega$ with $\delta\omega$ denoting the relative quadratic Stark shift between the initial state $\mid g\rangle$ and the ponderomotive shift of the excited Rydberg states (compare with the general discussion in Sec. 1). Besides the threshold contributions $C_1(z)$ and $C_2(z)$ the characteristic kernel $A_{gg}(z)$ is determined by the (resonant part of the) self energy of the initial state $|g\rangle$, i.e.

$$\Sigma(z) = \sum_n \frac{\mid\langle n|\mathbf{d}\cdot\mathbf{E}_0|g\rangle\mid^2}{z-\epsilon_n} = -i\frac{\gamma}{2} - i\gamma\sum_{M=1}^{\infty}(e^{i2\pi(-2z)^{-1/2}}\chi)^M. \tag{30}$$

This self energy is characterized by the laser-induced depletion rate

$$\gamma \quad = \quad 2\pi \mid \langle \epsilon = 0 | \mathbf{d} \cdot \mathbf{E}_0 | g \rangle \mid^2 \tag{31}$$

of the initial state $|g\rangle$ and by the scattering matrix element

$$\chi \quad = \quad e^{i2\pi\mu} \tag{32}$$

which describes all effects arising from scattering of the Rydberg electron by the ionic core and from photon absorption (compare with Eq.(3)). The sum over M in Eq.(30) originates from the multiple returns of the Rydberg electron to the core region where the dominant contribution to the self energy comes from. With each of these returns the Rydberg electron of energy $z < 0$ accumulates a phase of magnitude $2\pi(-2z)^{-1/2}$ and with each traversal of the core region it accumulates a (complex) phase of magnitude $2\pi\mu$ due to scattering by the core and due to photon absorption. The laser-induced depletion rate γ, the imaginary part of the quantum defect β and the second order Stark shift $\delta\omega$ describe the influence of the laser field on the Rydberg electron. As these quantities depend on the laser intensity they are not affected by phase fluctuations of the laser field.

Master equations of the form of Eq.(25) with a self adjoint Lindblad operator are of general interest as phenomenological models of continuous quantum measurement processes (Braginsky and Khalili 1992). In this context Eq.(25) would model excitation of Rydberg and continuum states close to an ionization threshold by a classical, deterministic laser field in the presence of continuous measurement of the initial state $\mid g\rangle$. Thereby the inverse bandwidth $1/b$ would determine the mean time between successive measurements.

Some qualitative aspects of the time evolution of an excited Rydberg electron under the influence of a fluctuating laser field are apparent from the contour plots of Figs. 5 and 6 which refer to one-photon excitation of a hydrogen atom by linearly polarized laser light with $|g\rangle = |2s\rangle$. It is assumed that Rydberg states around $\overline{n} = (-2\overline{\epsilon})^{-1/2} = 80$ are excited. According to the general discussion in Sec. 1 (compare with Eq.(4)) the laser-induced transitions from the excited Rydberg states to continuum states well above threshold are described by an imaginary quantum defect with $\beta = 0.00375\gamma$.

In Fig. 5a both the bandwidth of the laser field b and the field-induced depletion rate γ of state $\mid g\rangle$ are assumed to be small in comparison with the mean level spacing of the excited Rydberg states, i.e. $b, \gamma \ll \overline{n}^{-3}$. Thus, one may be tempted to think that this excitation process can be described well within the framework of a two-level approximation in which only states $|2s\rangle$ and $|80p\rangle$ are taken into account. However, Fig. 5a demonstrates that this expectation is only valid for sufficiently small interaction times. Indeed, the early stages of the excitation process are dominated by Rabi oscillations of the electron between the initial and the resonantly excited state. These Rabi oscillations are damped by the fluctuating laser field. An equilibrium is attained for interaction times

$t \geq 1/b$ for which all coherence between the two resonantly coupled states is negligibly small and for which $\rho_{gg}(t) \approx \rho_{\overline{nn}}(t) \approx 1/2$. This characteristic, well known two-level behavior is exemplified in Fig. 5a by the stationary probability distribution of the excited Rydberg state. (The probability distribution of state $|g\rangle$ which is localized in a region of a few Bohr radii around the nucleus is not visible on the radial scale of Fig. 5a). Fig. 5a indicates that for interaction times which are larger than a critical time t_1 this simple picture of the two-level approximation breaks down and the probability distribution of the excited Rydberg electron starts to spread towards larger distances from the core. (here $t_1 \approx 5 \times 10^5 T$ with $T = 2\pi\overline{n}^3$ denoting the mean classical orbit time). Simultaneously the probability distribution becomes more and more spatially de-localized with all nodes disappearing. In order to obtain a more detailed understanding of this diffusion-like process the time evolutions of the initial state probability and of the ionization probability are shown in Fig.5b . From Fig.5b it is apparent that this spatial spreading of the Rydberg electron is connected with a diffusion in energy space towards the ionization threshold. At interaction times $t \geq t_c \approx 7 \times 10^9 T$ the Rydberg electron has reached the ionization threshold and the ionization probability $P_{ion}(t)$ rises significantly from a negligibly small value to a value close to unity. Simultaneously the initial state probability $P_{gg}(t)$ starts to decrease faster. This stochastic diffusion of the Rydberg electron which eventually leads to ionization is a characteristic phenomenon brought about by the fluctuations of the exciting laser field. With the help of the theoretical approach presented above this characteristic stochastic ionization process can be analyzed in detail. Thus it can be shown (Alber and Eggers 1997) that the diffusion of the Rydberg electron towards the ionization threshold starts at time

$$t_1 = \frac{8}{\pi b \gamma T} \tag{33}$$

and eventually leads to stochastic ionization at interaction times $t \geq t_c$ with

$$t_c = \frac{4\pi}{\sqrt{27}\gamma b}\left[\frac{(\overline{\epsilon}^2 + 3(b^2 + \gamma^2/4)/4)^{3/2}}{\overline{\epsilon}^2 + b^2 + \gamma^2/4}\right]^{1/2}. \tag{34}$$

The time evolution of $P_{gg}(t)$ is approximately given by

$$P_{gg}(t) = \frac{2}{\sqrt{\pi}}[2b\gamma T]^{-1/2} t^{-1/2} \tag{35}$$

for $t_1 < t < t_c$ and crosses over to the power law

$$P_{gg}(t) = \frac{(\gamma + 2b)^2}{(2b\gamma\varphi/\pi)^2}\left[\frac{\gamma b \Gamma^3(5/3)}{27\pi(\overline{\epsilon}^2 + b^2 + \gamma^2/4)}\right]^{1/3} t^{-5/3} \tag{36}$$

for interaction times $t > t_c$. The variable φ characterizes the distance of the mean excited energy $\overline{\epsilon}$ from the ionization threshold and is determined by the

relation $-\overline{\epsilon} + i(b + \gamma/2) = Re^{i\varphi}$ $(0 \leq \varphi < \pi)$. At times $t \geq t_c$ the ionization probability rises according to the power law

$$P_{ion}(t) = 1 - \frac{\pi\Gamma(2/3)(\gamma + 2b)}{6b\gamma\varphi}[\frac{\gamma b}{\pi(\overline{\epsilon}^2 + b^2 + \gamma^2/4)}]^{1/3} t^{-2/3}. \qquad (37)$$

These approximate time evolutions are indicated by the dashed curves in Fig. 5b. The analytical results of Eqs.(33) and (34) explicitly show how the critical times t_1 and t_c for the breakdown of the two-level approximation and for stochastic ionization depend on the characteristic parameters of the problem, namely the mean excited energy $\overline{\epsilon}$, the laser bandwidth b and the laser-induced depletion rate of the initial state γ.

In Fig. 6 both the laser bandwidth and the laser-induced depletion rate of the initial state $|g\rangle$ are larger than the mean level spacing $\overline{n}^{-3}$ of the excited Rydberg states. As in this case the initial state is depleted by the laser field in a time which is small in comparison with the mean Kepler period of the excited Rydberg states, i.e. $1/\gamma \ll T = 2\pi\overline{n}^3$, an electronic Rydberg wave packet is prepared by power broadening (Alber and Zoller 1988). The initial stage of the preparation of this electronic wave packet by power broadening manifests itself in an approximately exponential decay of $P_{gg}(t)$ with rate γ. The repeated returns of fractions of this wave packet to the core region give rise to recombination maxima of $P_{gg}(t)$ which occur roughly at multiples of the mean Kepler period T. In the absence of laser fluctuations the non-perturbative time evolution of such an electronic wave packet under the influence of a laser field is already well understood. In the completely coherent case with each return to the core region a fraction of the electronic wave packet can be scattered resonantly in the presence of the laser field by stimulated emission and reabsorption of a laser photon accompanied by an electronic transition to the initial state $|g\rangle$ and back again. This emission and reabsorption process of a laser photon causes a time delay of the electronic wave packet of the order of $1/\gamma$ with respect to un-scattered fractions of the electronic wave packet. These repeated scattering processes lead to a splitting of the original wave packet into many partially overlapping fractions. In the completely coherent case the interference of these overlapping fractions inside the core region eventually give rise to a complicated time dependence of $P_{gg}(t)$ (Alber and Zoller 1991).

Characteristic qualitative aspects of the time evolution of an electronic wave packet in the presence of laser fluctuations are apparent from Fig. 6a. Clearly, the initial stages of the time evolution are dominated by the preparation of the electronic wave packet and by its repeated returns to the core region. However, at sufficiently long interaction times eventually the spatially localized electronic wave packet starts to spread out uniformly over the whole classically accessible region. Furthermore, this classical region starts to grow monotonically with increasing interaction time. Characteristic quantitative details of this time evolution are apparent from Fig. 6b. For sufficiently small interaction times the familiar recombination maxima of the repeated returns of the electronic wave

packet to the core region are clearly visible. However, as the coherence time of the laser field is small in comparison with the mean Kepler period, i.e. $1/b \ll T$, interferences between probability amplitudes which are associated with repeated returns to the core region are destroyed. Thus the details of the early stages of the time evolution of this electronic wave packet appear to be much simpler than in the completely coherent case. As a consequence of the diffusion of the electronic wave packet at longer interaction times the recombination maxima of $P_{gg}(t)$ disappear and merge into the power law of Eq.(35). At interaction times larger than t_c stochastic ionization of the Rydberg electron becomes significant and the power law decay of $P_{gg}(t)$ crosses over to the decay law of Eq.(36). Simultaneously the ionization probability rises to a value close to unity according to the approximate power law of Eq.(37).

In general stochastic ionization originating from laser fluctuations will compete with other coherent ionization mechanisms such as autoionization. As a consequence a number of new interesting phenomena are expected to arise which are not yet explored. In order to obtain first insights into basic aspects of this competition let us generalize our previous model to one-photon excitation of an autoionizing Rydberg series (Eggers and Alber 1998). Thus, it will be assumed that the laser excited autoionizing Rydberg series can be described within the framework of quantum defect theory in a two-channel approximation. In particular, let us concentrate on a case in which the fluctuating laser field excites Rydberg states close to an ionization threshold of an excited state of the ionic core (channel one) which can autoionize into channel two. For simplicity let us assume that direct excitation of channel two from the initial state $|g\rangle$ is not possible and that the effectively excited energy interval $(\overline{\epsilon}-b, \overline{\epsilon}+b)$ also covers continuum states of channel one. The early stages of this ionization process will be governed by an exponential decay of the initial state $|g\rangle$ with the laser-induced depletion rate γ, by autoionization of the excited Rydberg states of channel one into channel two, and by direct laser-induced ionization into the continuum states of channel one. As long as stochastic ionization is negligible, i.e. for interaction times t with $1/\gamma < t < t_c$, this ionization process will reach a metastable regime. Thereby the probability of ionizing into channel one is simply determined by the part of the effectively excited energy interval $(\overline{\epsilon}-b, \overline{\epsilon}+b)$ which is located above the ionization threshold, ϵ_1, of channel one. However, as soon as $t > t_c$ it is expected that the branching ratio between channels one and two is changed. For interaction times $t > t_c$ all Rydberg states whose autoionization lifetimes exceed the stochastic ionization time, i.e. $1/\Gamma_n > t_c$ (Γ_n is the autoionization rate of Rydberg state $|n,1\rangle$), will no longer autoionize into channel two but will eventually ionize stochastically into channel one. Thus for interaction times $t > t_c$ it is expected that the probability of ionizing into channel one is determined by the part of the effectively excited energy interval $(\overline{\epsilon}-b, \overline{\epsilon}+b)$ which is located above an energy of the order of $\epsilon_1 - 1/t_c$. Thus stochastic ionization is expected to lead to an effective lowering of the ionization threshold ϵ_1 of channel one. This manifestation of the competition

between autoionization and stochastic ionization is clearly apparent from Fig. 7 where the time evolution of $P_{gg}(t)$ is depicted together with the corresponding time evolutions of $P_{ion-ch1}(t)$ and $P_{ion-ch2}(t)$. In the case depicted in Fig. 7 the laser induced depletion rate γ is so small that no electronic Rydberg wave packet is prepared by power broadening. However, due to the large laser bandwidth, i.e. $bT \gg 1$, many Rydberg states are involved in the excitation process. This implies that to a good degree of approximation initially state $|g\rangle$ decays exponentially with rate γ.

Financial support is acknowledged by the Deutsche Forschungsgemeinschaft within the Schwerpunktprogramm 'Zeitabhängige Phänomene in Quantensystemen der Physik und Chemie'

References

Agarwal, G. S. (1976) Phys. Rev. Lett. **37**, 1383.
Alber, G., and Zoller, P. (1988) Phys. Rev. A **37**, 377.
Alber, G. (1989) Z. Phys. D **14**, 307.
Alber, G., and Zoller, P. (1991) Phys. Rep. **199**, 231.
Alber, G. (1992) Phys. Rev. Lett. **69**, 3045.
Alber, G., and Strunz, W. T. (1994), Phys. Rev. A **50**, R3577.
Alber, G., Strunz, W. T., and Zobay, O. (1994) Mod. Phys. Lett. B **8**, 1461.
Alber, G., and Eggers, B. (1997) Phys.Rev. A **56**, 820.
Aymar, M., Greene, C. H., and Luc-Koenig, E. (1996) Rev. Mod. Phys. **68**, 1015.
Beims, M. W., and Alber, G. (1993) Phys.Rev. A **48**, 3123.
Beims, M. W., and Alber, G. (1996) J. Phys. B **29**, 4139.
Braginsky, V. B., and Khalili, F. Ya. (1992) *Quantum Measurement*, Cambridge University Press, Cambridge.
Cooke, W. E., Gallagher, T. F., Edelstein, S. A., and Hill, R. M. (1978) Phys. Rev. Lett. **40**, 178.
Dando, P. A., Monteiro, T. S., Delande, D., and Taylor, K. T. (1995) Phys.Rev. Lett **74**, 1099.
Delos, J. B. (1986) Adv. Chem. Phys. **65**, 161.
Dixit, S. N., Zoller, P., and Lambropoulos, P. (1980) Phys. Rev. A. **21**, 1289.
van Druten, N. J., and Muller, H. G. (1995) Phys. Rev. A **52**, 3047.
Eggers, B., and Alber, G. (1998) (in preparation)
Fano, U., and Rau, A. R. P. (1986) *Atomic Collision and Spectra*, Academic, New York.
Gallagher, T. (1994) *Rydberg Atoms*, Cambridge University Press, Cambridge.
Garraway, B. M., and Suominen, K. A. (1995) Rep. Prog. Phys. **58**, 365.
Giusti-Suzor, A., and Zoller, P. (1987) Phys. Rev. A **36**, 5178.
Haken, H.(1970) in *Handuch der Physik* (S. Flügge, ed.) Vol. XXV/2c, Springer, Berlin.
Grobe, R., and Eberly, J. H. (1993) Phys. Rev. A **48**, 623 (1993)

Hanson, L. G., and Lambropoulos, P. (1995) Phys. Rev. Lett. **74**, 5009.
Hüpper, B., Main, J., and Wunner, G. (1995) Phys. Rev. Lett. **74**, 2650.
Jones, R. R., and Bucksbaum, P. H. (1991) Phys. Rev. Lett. **67**, 3215
Klöden, P. E., and Platen, E. (1992) *Numerical Solution of Stochastic Differential Equations*, Springer, Berlin.
Knospe, O., and Schmidt, R. (1996) Phys. Rev. A. **54**, 1154.
Koch, M., von Plessen, G., Feldmann, J., and Goebel, E. O. (1996) J. Chem. Phys. **120**, 367.
Landau, L. D., and Lifshitz, E. M. (1975) *The Classical Theory of Fields*, p. 181ff, Pergamon, Oxford.
Lankhuijzen, G. M., and Noordam, L. D. (1996) Phys. Rev. Lett. **76**, 1784.
Main, J., Wiebusch, G., Welge, K. H., Shaw, J., and Delos, J. B. (1994) Phys. Rev. A **49**, 847.
Moser, I., Mota- Furtado, F., O'Mahony, P. F., and dos Santos, J. P. (1997) Phys. Rev. A **55**, 3724.
Maslov, V. P., and Fedoriuk, M. V. (1981) *Semiclassical Approximation in Quantum Mechanics*, Reidel, Boston.
Mollow, B. R. (1975) Phys. Rev. A **12**, 1919.
Robicheaux, F. (1993) Phys. Rev. A **47**, 1391.
Seaton, M. J.(1983) Rep. Prog. Phys. **46**, 167.
Sepulveda, M. A., and Grossmann, F. (1996) Adv. Chem. Phys. **XCVI**, 191.
Stapelfeldt, H., Papaioannou, D. G., Noordam, L. D., and Gallagher, T. F. (1991) Phys. Rev. Lett. **67**, 3223
Vemuri, G., Anderson, M. H., Cooper, J., and Smith, S. J. (1991) Phys. Rev. A **44**, 7635.
Zobay, O., and Alber, G. (1995) Phys. Rev. A **52**, 541.
Zobay, O., and Alber,G. (1996) Phys. Rev. A **54**, 5361.
Zobay, O., and Alber, G. (1998) Prog. Phys. **46**, 3.

Figure 1: Schematic representation of the characteristic spatial regions which determine the dynamics of a Rydberg electron. Some classical trajectories which are relevant for the semiclassical wave function are also indicated.

Figure 2: Schematic representation of a laser-induced isolated core excitation process in Mg. After initial preparation in a $|3snd\rangle$ Rydberg state a second laser pulse excites the core $3s \rightarrow 3p$ transition. The Rydberg states of the excited core autoionize.

Figure 3: Three-channel excitation scheme including spontaneous emission process and autoionization.

Figure 4: Autoionization and resonant excitation of the core under the condition of period matching , i.e. $T_{orb} = T_{Rabi}$. The parameters are $\kappa^{-1} = 7$ns, $\overline{\nu}_1 = [-2(\epsilon - \epsilon_{c1})]^{-1/2} = 73$ ($T_{orb} = 59$ps), $\mu_1 = 0.0$, $\mu_2 = 0.5 + i0.1$, $\tau_a = 0.4 T_{orb}$ with $\mathcal{E}_a(t) = \mathcal{E}_a^{(0)} e^{-4(t-t_a)^2 \ln/\tau_a^2}$. Fig. 4a: Scaled ionization rate $\tilde{\gamma}(t) = \gamma(t) T_{orb} \tau_a / \mid \mathcal{D}_{g\mathbf{e}_a}^{(-)} \mathcal{E}_a^{(0)} \mid^2$ as obtained from the optical Bloch equations (full curve); Figs. 4b and 4c: Scaled zero- and one-photon contributions $\tilde{\gamma}^{(0)}(t)$ and $\tilde{\gamma}^{(1)}(t)$. (Reprinted from Zobay and Alber (1996), copyright 1998 by the Amercian Physical Society)

Figure 5: Excitation of an isolated Rydberg state: Radial contour plot (a) and $P_{gg}(t)$, $P_{ion}(t)$ (b) as a function of the interaction time t in units of the mean Kepler period T. The parameters are $\overline{n} = (-2\overline{\epsilon})^{-1/2} = 80$ ($T = 78$ps), $\gamma T = 0.1$, $bT = 0.01$. Various approximate asymptotic time dependences are also indicated, namely Eq.(35) (short dashed) and Eqs.(36) and (37) (long dashed).

Figure 6: Excitation of an electronic Rydberg wave packet by laser-induced power broadening: Radial contour plot (a) and $P_{gg}(t)$, $P_{ion}(t)$ (b) as a function of the interaction time t in units of the mean Kepler period T. The parameters are $\overline{n} = (-2\overline{\epsilon})^{-1/2} = 80$ ($T = 78$ps), $\gamma T = 10.0$, $bT = 10.0$. Various approximate asymptotic time dependences are also indicated, namely Eq.(35) (short dashed) and Eqs.(36) and (37) (long dashed). $\gamma t = 10.0$, $bT = 10.0$.

Figure 7: Competition between autoionization and stochastic ionization: Time evolution of $P_{gg}(t)$ and of the ionization probabilites into channels one and two $P_{ion-ch1}(t)$ and $P_{ion-ch2}(t)$. The parameters are $\overline{n} = \alpha_1 + (-2\overline{\epsilon})^{-1/2} = 80$, $\alpha_1 = 0.1$, $\gamma T = 1.0$, $bT = 300.0$, $\Gamma_n = 2\tau(n - \alpha_1)^{-3}/\pi$ with $\tau = 10^{-5}$ a.u. .

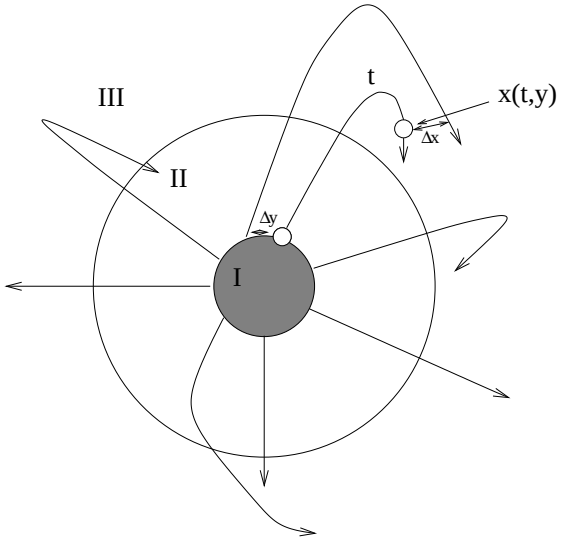
III
II
I
t
x(t,y)
Δx
Δy

1

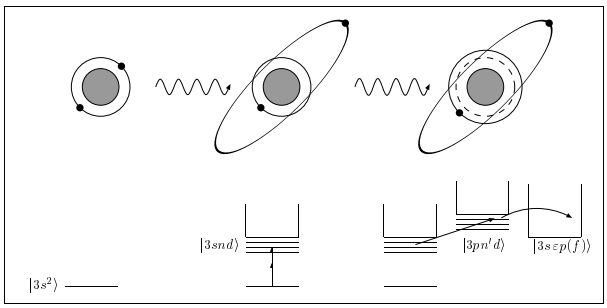

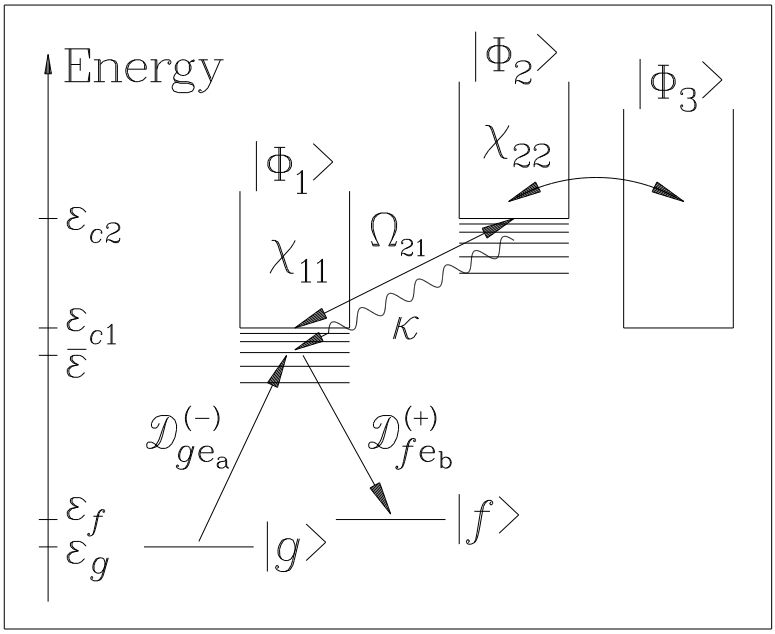
Energy
$|\Phi_2\rangle$
$|\Phi_3\rangle$
χ_{22}
$|\Phi_1\rangle$
ε_{c2}
Ω_{21}
χ_{11}
ε_{c1}
$\bar{\varepsilon}$
κ
$\mathscr{D}^{(-)}_{g\mathrm{e_a}}$
$\mathscr{D}^{(+)}_{f\mathrm{e_b}}$
ε_f
ε_g
$|g\rangle$
$|f\rangle$

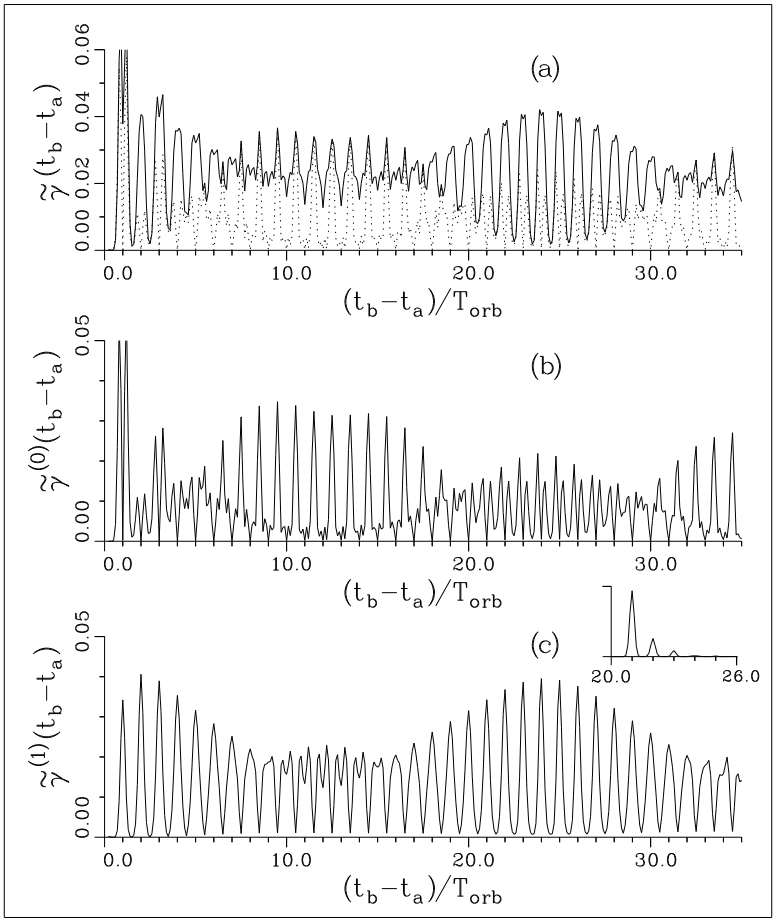
(a)
(b)
(c)
$\tilde{\gamma}(t_b-t_a)$
$\tilde{\gamma}^{(0)}(t_b-t_a)$
$\tilde{\gamma}^{(1)}(t_b-t_a)$
$(t_b-t_a)/T_{orb}$
0.00
0.02
0.04
0.06
0.05
0.0
10.0
20.0
30.0
26.0

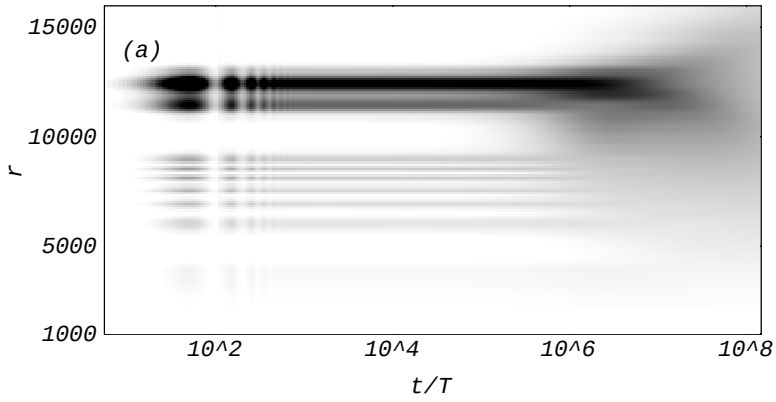
15000
(a)
10000
r
5000
1000
10^2
10^4
10^6
10^8
t/T

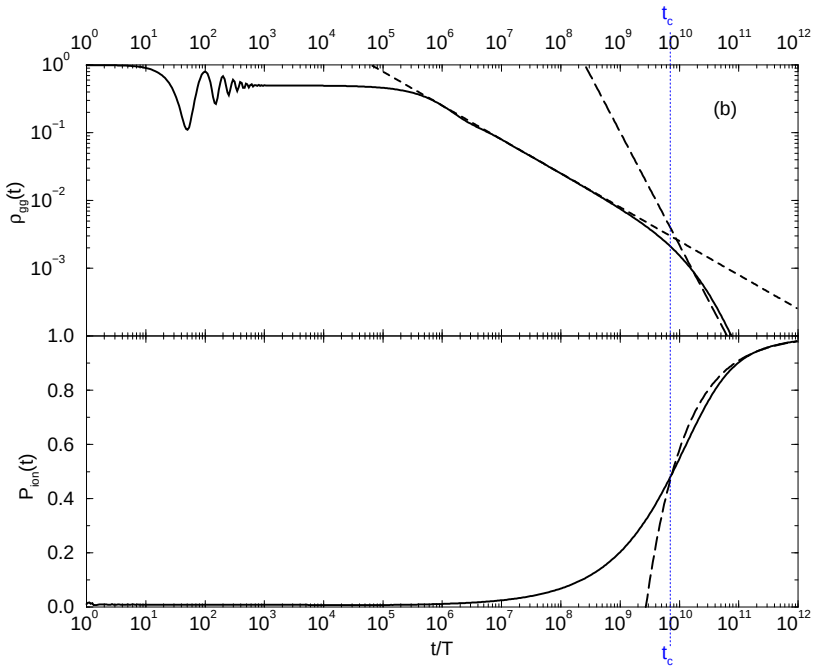
t_c
(b)
ρ_gg(t)
P_ion(t)
t/T
t_c

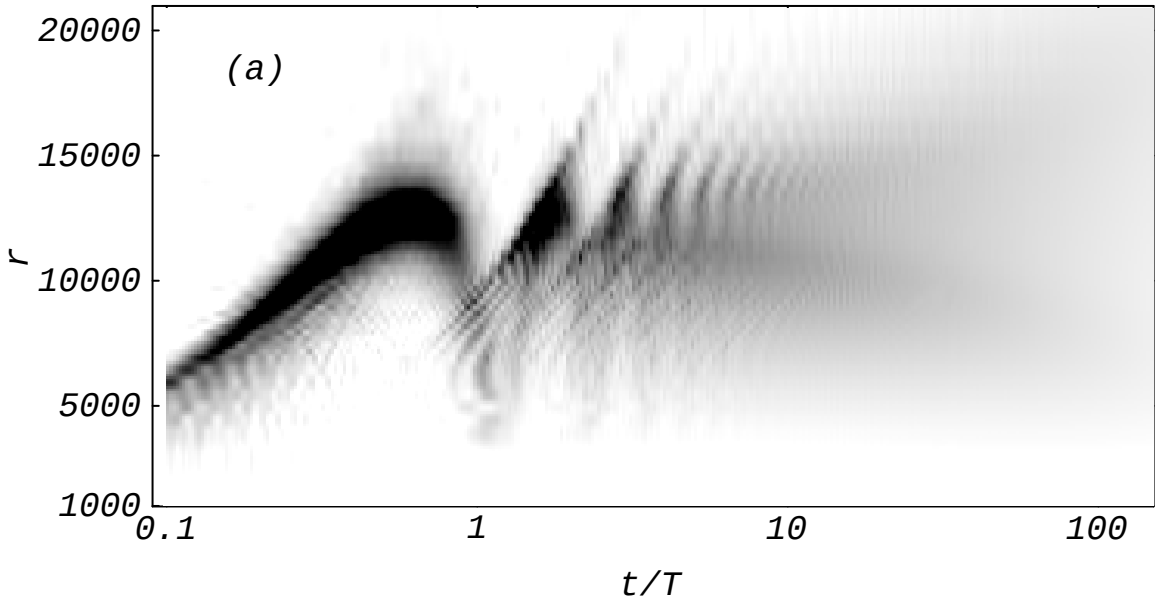
(a)
20000
15000
10000
5000
1000
r
0.1
1
10
100
t/T

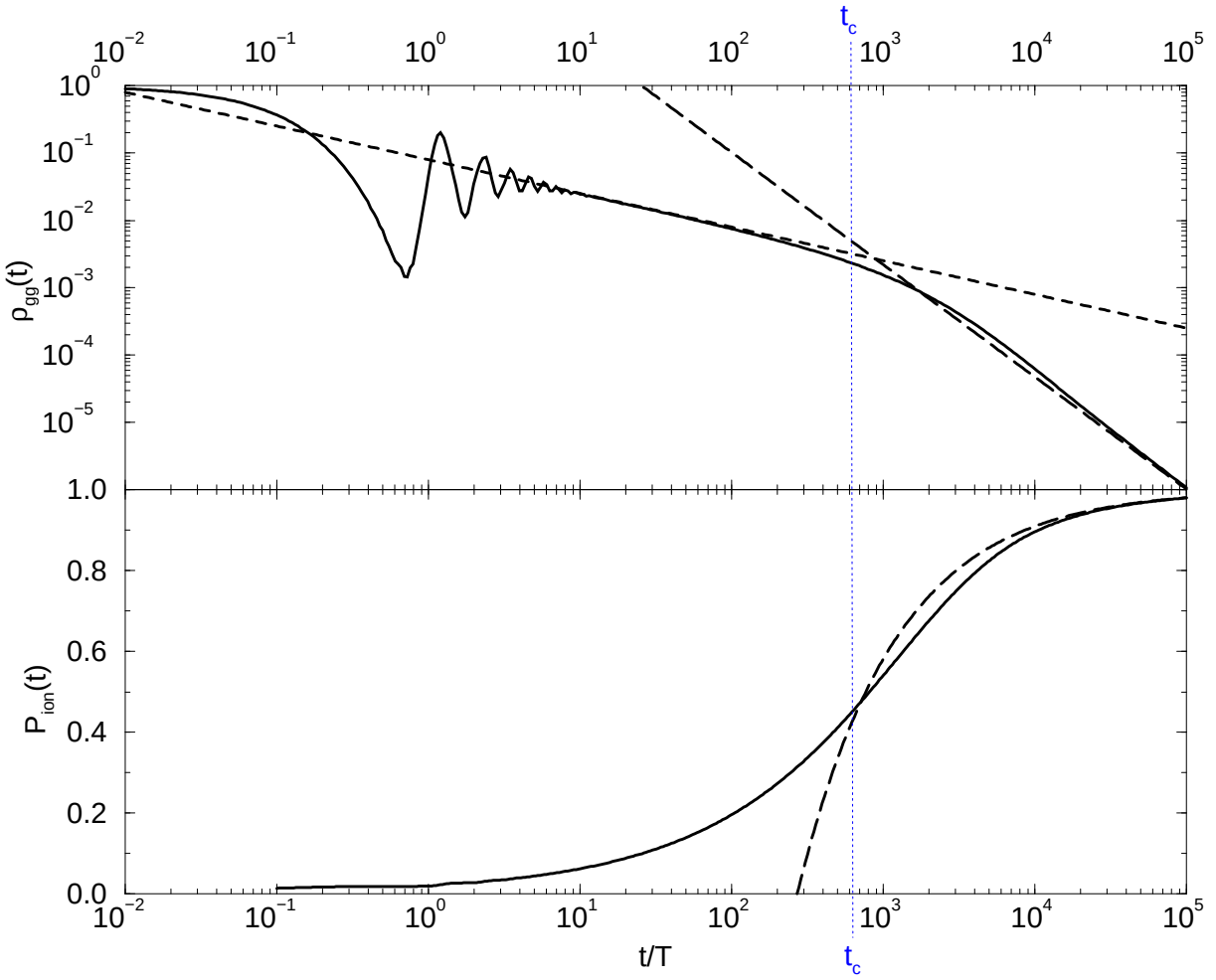
t_c
10^-2
10^-1
10^0
10^1
10^2
10^3
10^4
10^5
10^0
10^-1
10^-2
10^-3
10^-4
10^-5
ρ_gg(t)
1.0
0.8
0.6
0.4
0.2
0.0
P_ion(t)
t/T
t_c